

## Supporting Information

### High-Resolution Light-Activated Electrochemistry on Amorphous Silicon-Based Photoelectrodes

Shreedhar Gautam,<sup>a</sup> Vinicius R Gonçales,<sup>\*a</sup> Rafael N. P. Colombo,<sup>b</sup> Wenxian Tang,<sup>a</sup> Susana I. Córdoba de Torresi,<sup>b</sup> Peter J Reece,<sup>c</sup> Richard D. Tilley<sup>ad</sup> and J. Justin Gooding<sup>\*a</sup>

---

<sup>a</sup>. *School of Chemistry, Australian Centre of NanoMedicine and the ARC Centre of Excellence in Convergent Bio-Nano Science and Technology, The University of New South Wales, Sydney 2052, Australia. E-mail: [v.goncales@unsw.edu.au](mailto:v.goncales@unsw.edu.au); [justin.gooding@unsw.edu.au](mailto:justin.gooding@unsw.edu.au)*

<sup>b</sup>. *Instituto de Química, Universidade de São Paulo, Av. Prof. Lineu Prestes 748, 05508-080 São Paulo, SP, Brazil*

<sup>c</sup>. *School of Physics, The University of New South Wales, Sydney, 2052, Australia.*

<sup>d</sup>. *Electron Microscope Unit, Mark Wainwright Analytical Centre, The University of New South Wales, Sydney, 2052, Australia.*

## Experimental Methods

### Chemicals and Materials.

Hydrofluoric acid (Riedel-de Haën, 48 wt % solution), hydrogen peroxide (Sigma-Aldrich, 30 wt % solution) and sulfuric acid (J. T. Baker, 96 wt % solution) were all of semiconductor grade. 1,8-nonadiyne was redistilled from sodium borohydride (Sigma-Aldrich, 99 %) at lower pressure (65 – 70 °C, 25 – 30 torr) and kept in the argon atmosphere for further use. Copper sulfate pentahydrate was obtained from Chem Supply. All the solvents used for surface cleaning and modification were distilled before use. All aqueous electrolytes were prepared with Milli-Q water (>18 MΩ cm, Millipore, Australia) and were of analytical grade. Silicon wafers of prime grade polished single-sided p-type (boron-doped), (100) ± 0.5°, 500 – 550 μm thickness with resistivity of <0.003 Ω.cm and doping concentration of  $N_A \sim 1 \times 10^{19} \text{ cm}^{-3}$  were purchased from Siltronix Silicon Technologies (SST, France) referred in this article as pSi(100).

### Amorphous silicon-based heterojunctions.

Si (100) wafers were cut into small pieces of 2 X 2 cm<sup>2</sup> followed by rinsing with dichloromethane, dried with argon and dipped in Piranha solution (3:1 v/v ratio of sulfuric acid: hydrogen peroxide) for 10 minutes. Then, surfaces were rinsed with excess Milli-Q water before transferring to a HF solution (1:10 v/v HF: H<sub>2</sub>O, RTP) for 1 minute to etch silicon oxide. Next, surfaces were rinsed again with Milli-Q for 1 minute and dried with argon stream followed by amorphous silicon deposition. Realising that silicon oxide might reform if kept in ambient atmosphere for a long time, etched crystalline silicon was directly transferred into Oxford Instruments Plasmalab 100 plasma-enhanced chemical vapor deposition (PECVD) and intrinsic amorphous silicon was deposited. Amorphous silicon was deposited with the respective parameters; precursor SiH<sub>4</sub> (25 sccm, Coregas, 99.999%), carrier Ar (475 sccm, Coregas, 99.99999%), RF plasma (15 W, 13.56 Hz RF generator), 1000 mTorr and deposition temperature of 300 °C was used until thickness of 200 nm was reached.

### Functionalization of amorphous silicon surface with acetylene.

Amorphous silicon deposited on crystalline silicon were acetylated by covalent modification of 1,8-nonadiyne by following the previous protocol<sup>2</sup>. The samples were first rinsed with dichloromethane and dried under argon stream followed by cleaning in hot Piranha solution (3:1, v/v, concentrated sulfuric acid: 30 % hydrogen peroxide) for 30 minutes. Next, samples were again rinsed with excess Milli-Q water and etched with hydrogen fluoride solution (2.5 wt % aqueous solution) for 90 s to remove any aged silicon oxide. Wafers were then shifted to Schlenk flask with degassed 1,8-nonadiyne by at least five freeze and thaw cycles in argon atmosphere. The reaction occurred at 165 °C for 3 hours resulting in self-assembled alkyne-terminated monolayer on amorphous silicon surface. The surface was cleaned in dichloromethane at 4 °C for 12 hours to remove the unreacted reactants.

### Fabrication of photoresist patterns on acetylenylated amorphous silicon surface.

Photoresist (SU-8-2005, Microchemicals, Germany) was first spin coated at 4000 rpm for 30 s on alkyne-terminated crystalline/amorphous silicon surface followed by soft baking at 95 °C for 2 minutes. Then, the surface was irradiated with UV light with exposure energy of 100 mJ cm<sup>-2</sup> for 10 s using Karl suss MA6 mask aligner. Post exposure bake was performed at 95 °C for 2 minutes followed by development at SU-8 developer (Microchemicals, Germany) for 1 min and rinsed with isopropanol for 1 minute and subsequently, dried under nitrogen stream. In order to fabricate nanopatterns, e-beam lithography (Raith 150 TWO, Raith GmbH) was used. First, the wafer was baked at 110 °C for 5 min for dehydration followed by spin-coating with negative e-beam resist (ma-N 2403) at 3000 rpm for 30

s. Then, it was soft baked at 90 °C for 1 min. To pattern the surface, 10 kV acceleration voltage with an exposure dose of 50  $\mu$ C cm<sup>-2</sup> was used. Finally, the surface was developed with ma-D 525 developer for 45 s, rinsed by Milli-Q water for 3 min and blow dried with N<sub>2</sub> stream for further usage.

#### **Click-functionalization of ferrocene on patterned acetylenylated amorphous silicon surface.**

A previous published protocol was employed to synthesize azidomethylferrocene from ferrocenemethanol<sup>3</sup>. The patterned acetylene-terminated surfaces were clicked with azidomethylferrocene via click chemistry. For that, 100 mM sodium ascorbate in water, 10 mM azidomethylferrocene in isopropyl alcohol and 400  $\mu$ M CuSO<sub>4</sub> were added in volumetric ratio of 1:4:1, respectively. Then, the click reaction was conducted at dark in room temperature for 40 minutes. The surface was thoroughly rinsed with Milli-Q water, isopropanol, ethanol and 500 mM hydrochloric acid before performing further experiments. 500 mM hydrochloric acid was used to etch physisorbed copper species on the surface.

#### **X-ray photoelectron spectroscopy.**

ESCALab 250 Xi spectrometer (Thermo Scientific) was used for X-ray photoelectron spectroscopy (XPS) with a monochromatic Al K $\alpha$  source with the base pressure of  $<10^{-8}$  mbar. Advantage 4.73 software was used for used for the curve fitting and spectral analysis. All binding energies reported were calibrated to C 1s signal at 284.8 eV.

#### **Electrochemical Measurements.**

All the electrochemical measurements were performed in an electrochemical chamber of gasket ring sized 5.8 mm in diameter via CHI660D potentiostat. A conventional 3 electrode system was prepared with ferrocene modified silicon/amorphous silicon as working electrode, Ag|AgCl|1 M KCl as reference electrode and platinum as counter electrode. Ohmic contact at working electrode was made by attaching working electrode against copper plate to be connected to potentiostat with Ga-In eutectic mixture. The back side of silicon was scratched to remove the acetylene monolayer before the attachment. The chamber comprising of working electrode with patterns was stationed at Märzhäuser motorized stage (EK 75 X 50 Pilot, 00-27-351-0000) and the speed was controlled by the software to drive the patterns across light. A pigtailed laser diode of 642 nm (FT030-V, Thorlabs) connected to a temperature controller (ITC4001, Thorlabs) was used. A single optical fibre was attached to the collimator and the collimated light was focused with objective lens (40X magnification) of a microscope (Olympus BX53). The pattern was visualized with the microscope and the electrochemical measurements were run by moving the motorized stage with certain speed. The diameter of laser beam was determined with diminishing the intensity 10,000 times followed by the measurement with the line scan on microscope image. The image was also calibrated with known photolithographic pattern to confirm the accuracy. Calibration of power was conducted with PM 20D digital power and energy meter with S120C Si sensor (Thorlabs, USA). The power loss from penetration of light via electrolyte of 1 cm height was not considered to determine the power.

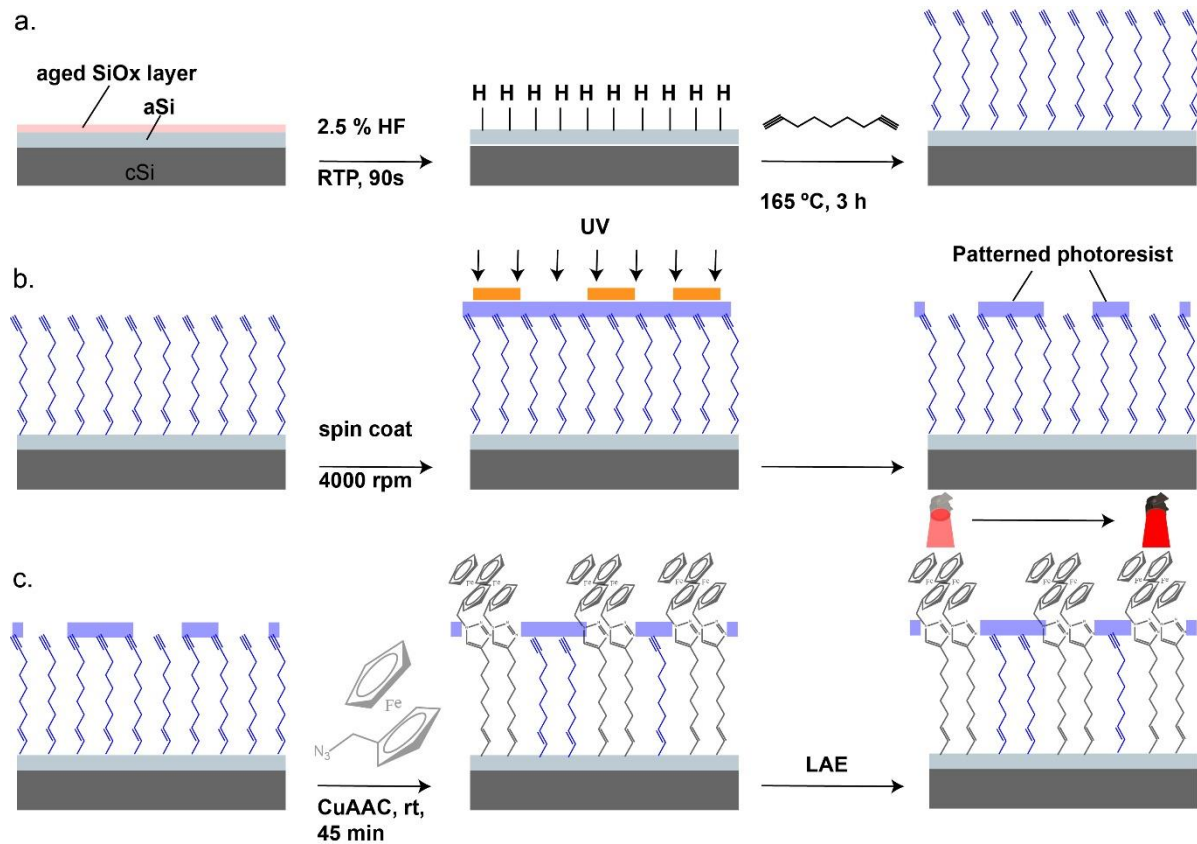


Figure S1. Schematic representation to illustrate the preparation of amorphous silicon-based surface used for determining the spatial resolution. (a) Thermal hydrosilylation was performed on hydrogenated amorphous silicon to form a self-assembled monolayer by grafting 1,8-nonadiyne. This thin organic monolayer based on  $\alpha,\omega$ -diynes confers surface stability on photoelectrodes for LAE which facilitates amperometric measurements; (b) A photolithographic method was used to pattern gaps of a photoresist on acetylenylated pSi(100)|aSi surface. The electrode was spincoated with photoresist followed by the exposure of UV light selectively blocked by photomask. The negative photoresist crosslinks after exposure with light (10 s) and the non-exposed one is dissolved to form the above pattern; (c) Functionalization of azidomethylferrocene via click chemistry only on the exposed acetylene-terminated area. Light beam was scanned on the patterned surface to measure the amperometric current and correlate the real width of photoresist gap to the electrochemically determined gap by light-activated electrochemistry (LAE).

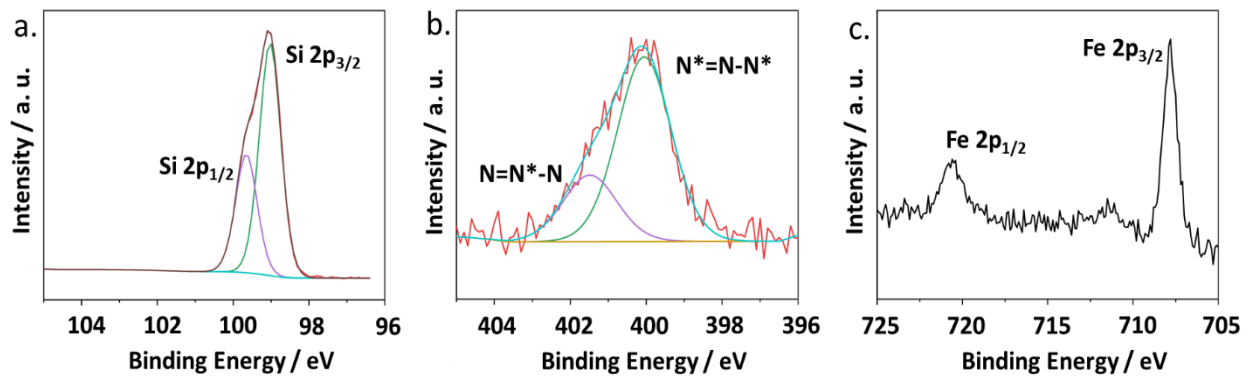


Figure S2. (a) XPS Si 2p narrow scan of amorphous silicon surface modified by 1,8-nonadiyne via thermal hydrosilylation. In the narrow scans of Si 2p<sub>1/2</sub> and 2p<sub>3/2</sub> peaks were observed at 99.5 and 100.1 eV. The absence of peak for silicon oxide within the range of 102-104 eV confirms the stability of the surface against oxidation<sup>1</sup>. Narrow scans of (b) N 1s and (c) Fe 2p. Acetylene terminated surface modification with azidomethylferrocene via copper(I)-catalysed azide-alkyne-cycloaddition was confirmed via N 1s spectra due to the presence of triazole ring N=N peaks at 400.2 and 401.8 eV in the ratio of 2:1 which confirms the click reaction. Furthermore, the presence of Fe 2p<sub>1/2</sub> and Fe 2p<sub>3/2</sub> confirms the surface modification with ferrocene.

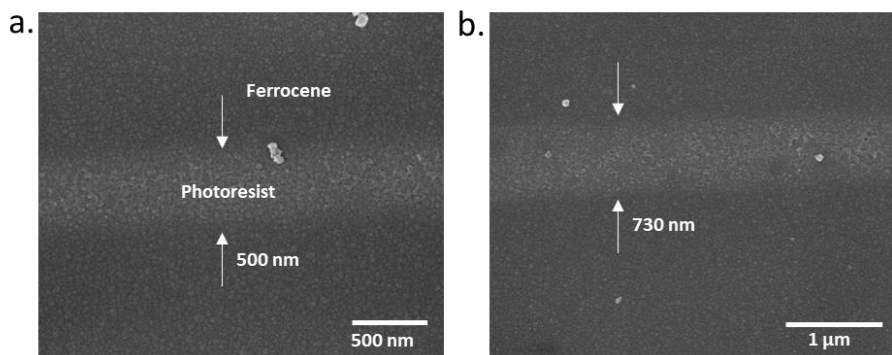


Figure S3. SEM images of photoresist gaps fabricated by e-beam lithography on pSi(100) | aSi electrode. Patterning was performed at 10 kV acceleration with the exposure dose of 50  $\mu\text{C cm}^{-2}$ . E-beam lithography was used for the patterns smaller than 1  $\mu\text{m}$  because of the 1  $\mu\text{m}$  resolution limitation of MA6 mask aligner.

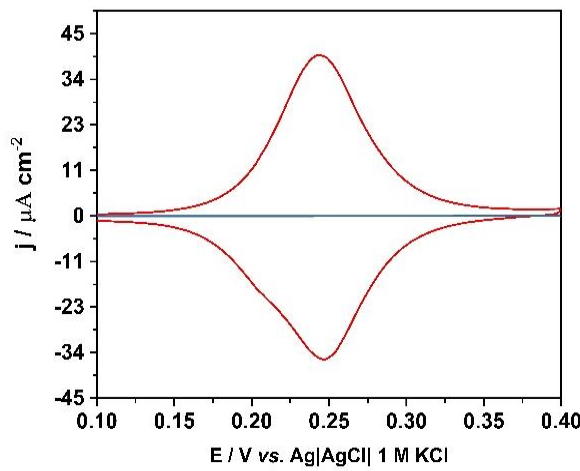


Figure S4. Cyclic voltammograms of ferrocene modified pSi(100)|a-Si in light (red) and dark (blue). The scan rate was 100 mV s $^{-1}$  and the electrolyte 1 M perchloric acid.

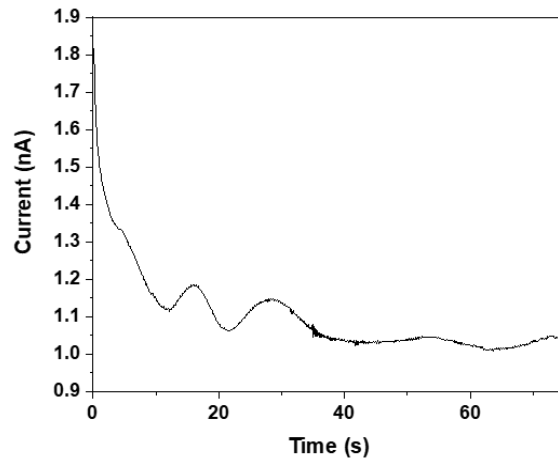


Figure S5. Amperometric trace showing the background current. The pSi(100)|aSi electrode was held at 0.25 V versus Ag|AgCl|1 M KCl in dark. The surface contains bound ferrocene. 1 mM ferrocyanide was used to recycle ferrocenium back to ferrocene and 100 mM KNO<sub>3</sub> was used as supporting electrolyte.

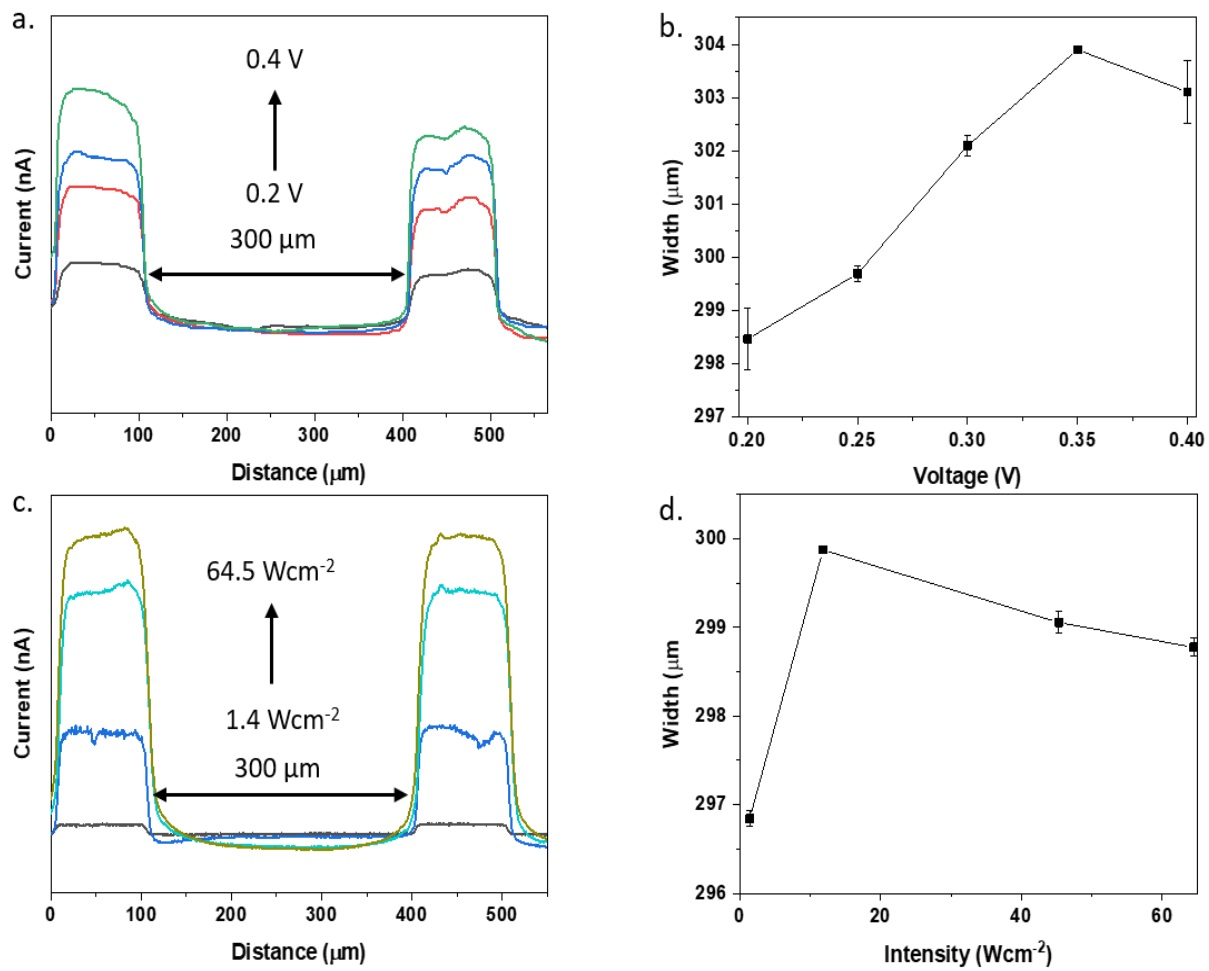


Figure S6. Variation of FWHM on pSi(100) | aSi with applied (a) potential and (b) light intensity. The light intensity was 11.8  $\text{W cm}^{-2}$  while electrode was biased at +0.20, +0.25, +0.30, +0.35 and +0.40 V vs Ag|AgCl|1 M KCl. The potential was 0.25 V vs Ag|AgCl|1 M KCl while varying the intensity with 2.2, 11.8, 45.3 and 64.5  $\text{W cm}^{-2}$ . The width of the gap was 300  $\mu\text{m}$ .

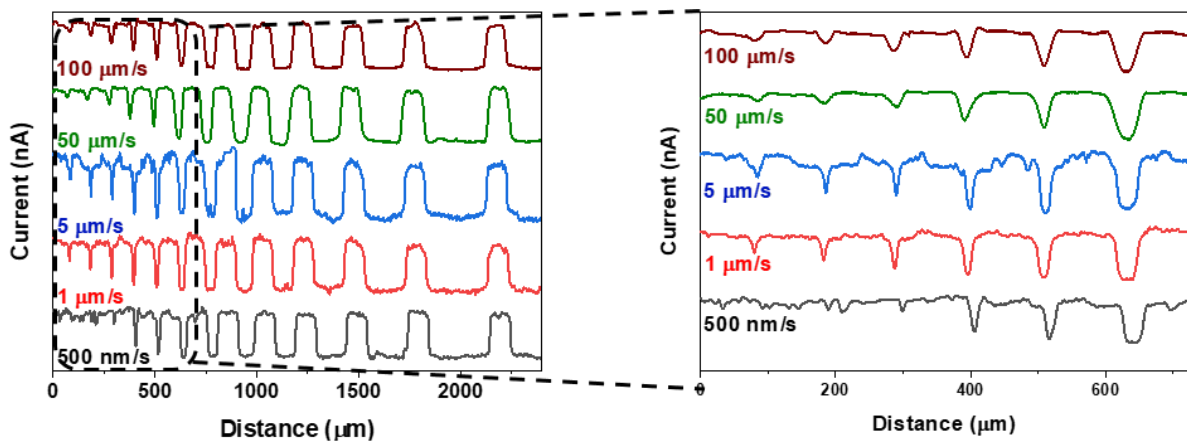


Figure S7. The features observed by varying the raster speeds of 500 nm  $\text{s}^{-1}$ , 1  $\mu\text{m s}^{-1}$ , 5  $\mu\text{m s}^{-1}$ , 50  $\mu\text{m s}^{-1}$  and 100  $\mu\text{m s}^{-1}$  and the enlarged figure on the right.

### Derivation of the model:

Assuming a mass transport-controlled system and constant homogeneous Nernstian diffusion layer, the charge will be obtained from the integration of the current-time profile:

$$\int dQ = -\frac{nFDC}{\delta} \int A(t)dt$$

For a circular light-beam illuminating the electroactive site:

$$A(t)_{max} = \pi r^2$$

$$Q(t) = -\frac{nFDC}{\delta} \pi r^2 \Delta t = Q_{max}$$

For a circular light-beam illuminating a completely non-active region:

$$Q(t) = Q_{min}$$

If the light-beam leaves an active site and a fraction of the area begins to illuminate a non-active region, the charge variation ( $Q_{loss}$ ), i.e. the difference in anodic charge compared to the fully electroactive area, is:

$$Q_{loss} = -\frac{nFDC}{\delta} \cdot \int \left( \overbrace{r^2 \cos^{-1} \left( \frac{r-vt}{r} \right)}^{A(t)} - (r-vt) \sqrt{2rvt - v^2 t^2} \right) dt$$

Where n, F, D, C,  $\delta$ , r, v and t are number of electrons transferred, Faraday constant, diffusion coefficient, concentration of redox species, thickness of the Nernstian diffusion layer, radius of light beam, rastering-speed of light beam and time respectively.

Measured charge is  $Q(t) = Q_{max} - Q_{loss}(t)$

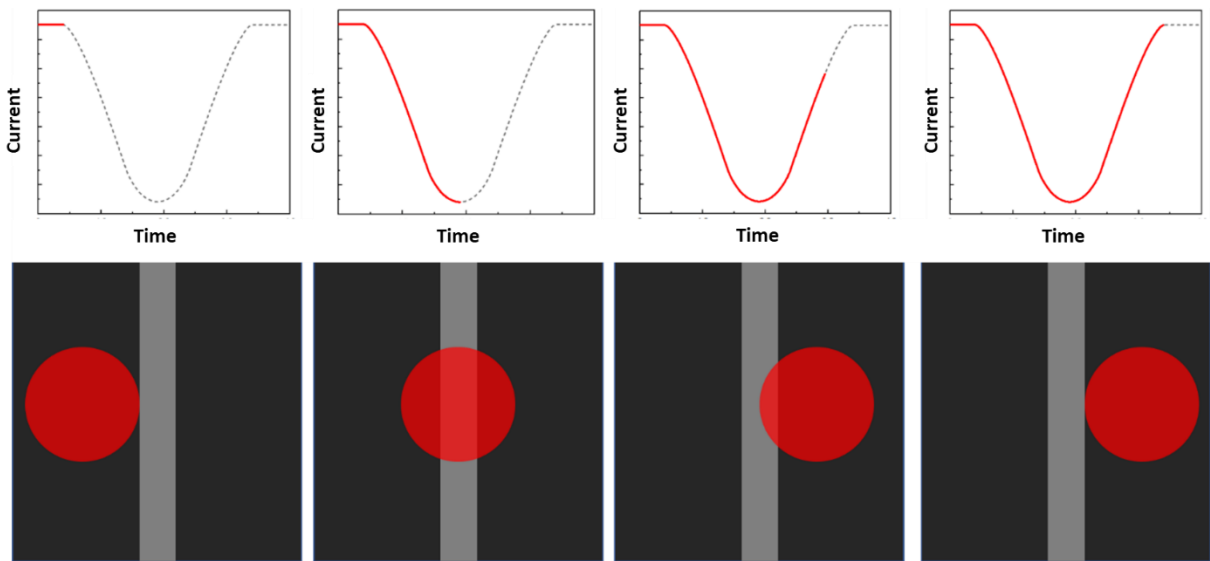
The smallest distinguishable trench that leads to a current difference ( $\Delta x_{min}$ ):

$$\Delta x_{min} = 3 * \frac{SD(Q_{max})}{\frac{dQ}{dL}} = 250 \text{ nm}$$

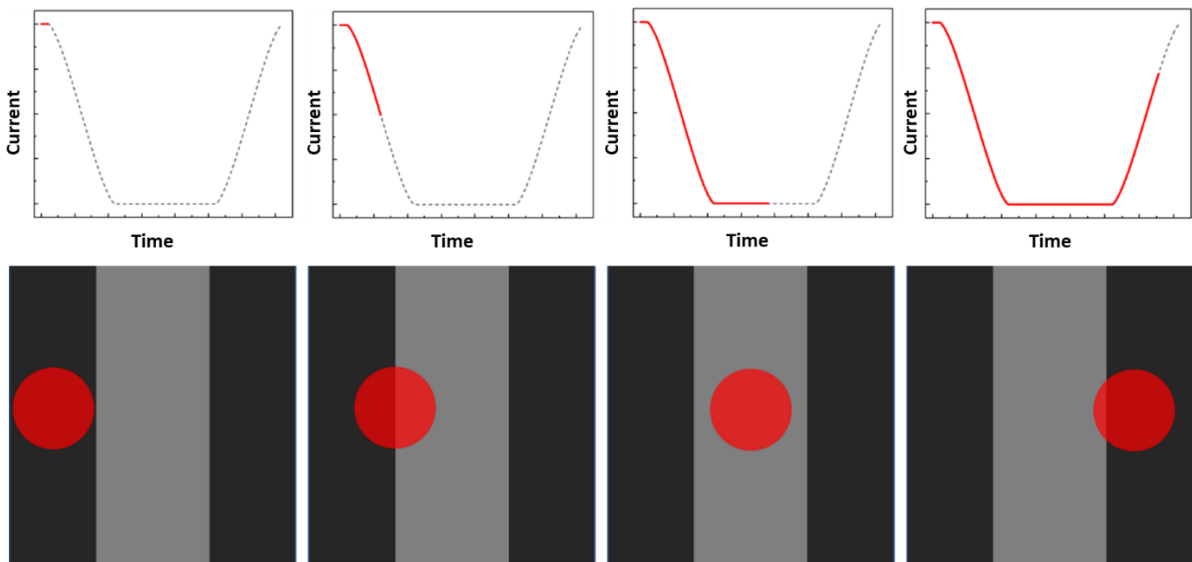
Where SD means is the standard deviation, Q is the charge-loss and L is the width of each gap

$A(t)$  is the area of light beam on the redox species as the function of time. When the circular Gaussian beam is on the ferrocene band at time "0 s",  $A(t)$  equals  $\pi r^2$  (area of full circle) and the total electrochemical charge is given by  $Q_{max}$ . As the beam moves towards the photoresist (gap), the light-beam is partially illuminated on the ferrocene band, thus partial current (Q is generated by the oxidation of ferrocene to ferrocenium. This decrement in charge  $Q(t)$  is the difference of  $Q_{max}$  and  $Q_{loss}$  which is the function of width (L) of each gap. Therefore, we can predict the width of photoresist gap electrochemically by corelating with  $Q(t)$ .

**When  $L < 2r$  (Gap size smaller than light-beam diameter)**



### When $L > 2r$ (Gap size larger than light-beam diameter)



### References

1. S. A. A. Ahmad, S. Ciampi, S. G. Parker, V. R. Gonçales and J. J. Gooding, *ChemElectroChem*, 2019, **6**, 211-220.
2. V. R. Gonçales, J. Lian, S. Gautam, D. Hagness, Y. Yang, R. D. Tilley, S. Ciampi and J. J. Gooding, *The Journal of Physical Chemistry C*, 2020, **124**, 836-844.
3. S. Ciampi, G. Le Saux, J. B. Harper and J. J. Gooding, *Electroanalysis*, 2008, **20**, 1513-1519.